Some Experimental Lessons on Digital Filtering in the ALADIN-France 3DVAR Based on Near-Ground Examination

CLAUDE FISCHER AND LUDOVIC AUGER

CNRM/GAME, Météo-France/CNRS, Toulouse, France

(Manuscript received 17 February 2010, in final form 10 September 2010)

ABSTRACT

This paper deals with the characteristics and effects of digital filter initialization, as implemented in the operational three-dimensional variational data assimilation (3DVAR) system of the Aire Limitée Adaptation Dynamique Développement International (ALADIN)-France regional weather forecast model.

First, a series of findings on the properties of the initialization of the model are discussed. Examples of initial spinup linked with inertia–gravity wave occurrence are shown, and the major sources for their generation are listed. These experimental results are compared with past and present experiences concerning the use and need for digital filter initialization. Furthermore, the impacts of switching to an incremental formulation of the filter in data assimilation mode are demonstrated. Second, the effects of the filter formulation on the results of an observation impact study are illustrated. The latter consists of implementing screen-level, 10-m horizontal wind information into the ALADIN 3DVAR analysis. There can, indeed, be some delicate interference between observation impact evaluation and the effects of filtering, at least on short-term forecasts.

The paper is concluded with some general considerations on the experimental evaluation of spinup and the link between the assimilation system design and model state filtering.

1. Introduction

The term spinup is usually used within numerical weather prediction (NWP) contexts in relation to two issues: 1) the experimental framework that consists of launching a coupled NWP model with initial conditions provided by a *different* coupler model (or any external gridded analysis procedure) and 2) the period of time from model launch during which all model fields undergo a process of adjustment before a discretized model equation compliant three dimensional (3D) state is achieved. The first of these issues leads to the definition of a ''spinup model,'' as opposed to a model run in assimilation mode, which would start using a background state obtained from a ''domestic'' forecast. In the Aire Limitée Adaptation Dynamique Développement International (ALADIN)-France community, the spinup model is also often called a dynamical adaptation model, when the limited area model (LAM) is started with a global uninitialized analysis coming from the Action de Recherche Petite Echelle Grande Echelle (ARPEGE) system. For general presentations of the global spectral model ARPEGE, we refer to Courtier et al. (1991) and Geleyn et al. (1995), and for its limited area, spectral bi-Fourier version ALADIN, we refer to Radnóti et al. (1995) or Horányi et al. (2006). Note that the lateral boundary coupling in ALADIN follows the classical relaxation method introduced by Davies (1976) and adapted to a spectral LAM by Haugen and Machenhauer (1993).

The second issue above is the one of concern in section 2 of this paper: the spinup period of an NWP model will be determined by the time taken by the model to adjust its initial fields with respect to all, discretized, model equations. This spinup generally contains processes of dynamical adjustment that are of a geostrophic type, with excess energy radiated away by inertia–gravity waves, and processes of diabatic adjustment, where model physics tendencies will converge with respect to other model forcings. Dynamical adjustment will for instance ensure that the low-level model wind field is in balance with the local discretized orography. Diabatic adjustment will ensure that water vapor and other microphysics species, as well as their related physics tendencies, are in balance with the local wind and temperature fields (e.g., convergence, vertical shear, vertical stability, etc.).

A first possible experimental framework for launching a (coupled) model therefore consists of letting the model

Corresponding author address: Claude Fischer, Météo-France/CNRM/GMAP, 42 Av. G. Coriolis, 31057 Toulouse, France.
E-mail: claude.fischer@meteo.fr

DOI: 10.1175/2010MWR3388.1

freely go through its spinup process, expecting no actual use of the first hours of the forecast since those will be affected by nonmeteorological waves and possibly excessive precipitation amounts. Alternatively, assuming that most of the adjustment will occur through rapid and high-frequency waves, as well as fairly short-term model tendencies, one may force the initial state not to generate any model tendencies that project onto high-frequency model solutions, using some type of initial state filtering. For instance, in nonlinear normal mode initialization (NNMI; Machenhauer 1977), the subspace of the high-frequency solutions is obtained from a simplified geophysical model, which is able to discriminate between Rossby and inertia–gravity modes. In the practical implementation of NNMI, the filtered initial state is obtained after a few iterations of the scheme, which leads to a reduction of the tendencies of the inertia–gravity wave modes. Another prominent method for filtering is digital filter initialization (DFI; Lynch 1990; Lynch and Huang 1992), where successive model time steps are computed and filtered by the means of a given response function.

In ALADIN, DFI has been implemented for the usage of the model in dynamical adaptation mode, following the diabatic DFI procedure introduced in Huang and Lynch (1993). Lynch (1997) introduces the Dolph–Chebyshev filter as a response function for providing an effectively optimal filter. Since then, most of our experimental knowledge about ALADIN spinup properties has been obtained by running the model in dynamical adaptation mode with DFI. We describe the most common digital filter application in the ALADIN model in the appendix, along with the definition of the parameters that will be discussed in this paper. Typical parameter choices for the DFI step are to run the filter over a 2.5-h time span with a stop-band edge period of 3 h. We usually consider that after this DFI the dynamical spinup process is marginal, while a diabatic adjustment still exists, over about 6–12 h. The first-order importance of the coupling between diabatic tendencies and vertical motion or convergence–divergence at the mesoscale has been illustrated in Pagé et al. (2007). The diabatic adjustment mostly is a consequence of the removal by DFI of part of the convergence–divergence patterns linked with active systems, and that could already be present in the ARPEGE analysis (despite its lower resolution compared with ALADIN, typically 15–20 versus 8–10 km), along with the necessary adaptation of physics processes to the higher-resolution discretization, and related forcings (surface heterogeneities, orography). This diabatic adjustment exists despite the almost identical physics parameterization packages used by ARPEGE and ALADIN-France in Météo-France's operational implementation, for instance.

When it comes to data assimilation, our experience with the ALADIN system remains, so far, fairly limited. We will come back in more detail to this aspect in section 2b. We stress that in our study, the model resolution is 9.5 km with 46 vertical levels, and the three-dimensional variational data assimilation (3DVAR) analysis increment is computed on the model grid and, thus, its resolution also is 9.5 km. The model time-step length is 415 s. The ALADIN 3DVAR does not contain any extra penalty function for filtering purposes (the so-called J_c term), and analysis increments primarily are constrained by the balance and multivariate specifications included in the background term J_b, following the work performed within the framework of the global model by Derber and Bouttier (1999) and within the framework of the LAM by Berre (2000). These specifications mostly consist of a statistically derived linear balance and the decomposition of the control vector of the variational problem into balanced and unbalanced parts. The formulation furthermore includes a horizontal scale dependency of vertical correlations for each unbalanced component.

This paper aims to illustrate three aspects of the preparation of the initial state for a model forecast: observation of spinup effects (inertia–gravity wave signals); revisiting the pros and cons of two versions of filtering, namely the nonincremental and the incremental ones (we refer to section 2b for the details); and assessing the sensitivity of observation impact studies to the filtering strategy. Our work is primarily of an experimental nature; we do not claim to have performed a thorough theoretical discussion on filtering or data assimilation. Our concern here is the discussion of a number of the results that we have obtained over time on those three items. The paper is organized as follows. Section 2 addresses several experimental findings concerning the spinup properties and filtering strategies in the ALADIN-France LAM. Section 2a specifically deals with the experimental evidence and study of some of the spinup waves. In section 2b, the consequences of the formulation of the filter and its tuning, in the case of digital filtering, are inferred and tested. We measure the impact in terms of conventional scores with respect to surface observations (where spinup effects are most visible). We continue with a discussion of the impacts of the filtering strategy within observation sensitivity experiments (OSEs), comparing incremental versus nonincremental applications of DFI (section 3). We draw several lessons from this work in section 4.

2. Spinup and digital filtering

a. Spinup as seen on short-term model forecasts

When the 3DVAR data assimilation was tested and implemented in the ALADIN-France system (see Fischer

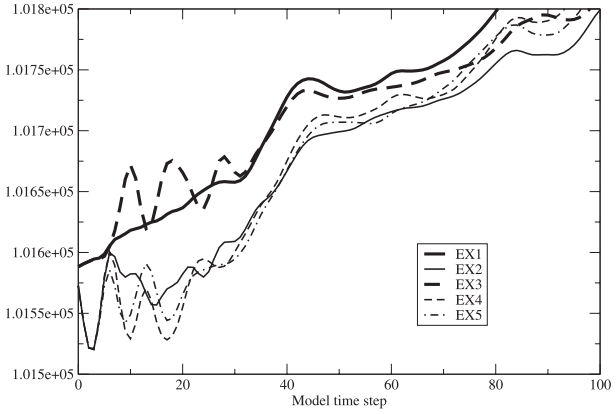

FIG. 1. Time series of surface pressure at a model grid point located in the Bay of Biscay for five experiments (see Table 1). Units are model time steps (horizontal axis, 1 h corresponds to about nine time steps) and Pa (vertical axis).

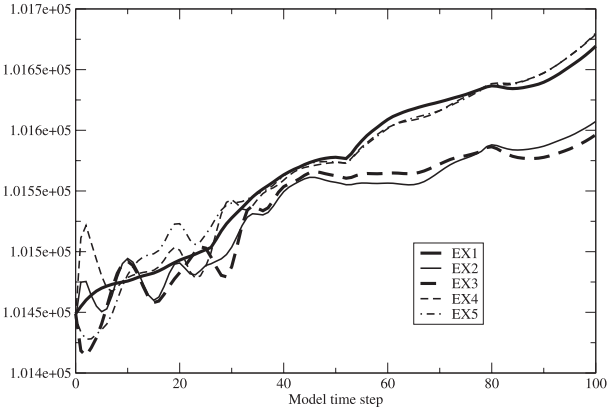

FIG. 2. Time series of surface pressure at a model grid point located 50 km inside the model's relaxation zone for five different experiments (see Table 1). Units are model time steps (horizontal axis, 1 h corresponds to about nine time steps) and Pa (vertical axis).

et al. 2005), the filtering of the initial state was kept the same as in the dynamical adaptation. On the one hand, we have considered that the move toward an assimilation cycle should introduce a smaller amount of spinup and a shorter spinup time, because the initial state (the analysis) then is the addition of a previous (here, 6-h lead time) forecast (as background) plus an analysis increment. The background 6-h forecast fields are in fairly good balance, as we will illustrate below. Some level of mass–wind balance furthermore is present in the increment, via statistical regression coefficients between predictors in the control vector of the 3DVAR following the works of Derber and Bouttier (1999) and Berre (2000). On the other hand, some trials to move away from the DFI specifications used in dynamical adaptation mode, mostly with the goal of diminishing the intensity of filtering the total 3DVAR analysis, lead to mitigated results: on the positive side, the very-short-term forecasts often exhibited a shorter diabatic adjustment time when filtering less; on the negative side, when for instance the stop-band edge period was decreased, we also found cases of spurious onsets of precipitations in nonactive areas. Thus, the decision was made to keep the DFI procedure within the assimilation identical to the dynamical adaptation mode. This choice amounted to starting any actual forecast, either within the assimilation cycle or for the parallel, long-term production runs, from the filtered analysis denoted as $f(a)$ henceforth, where a denotes the analysis.

After the first operational implementation of 3DVAR in ALADIN-France, we reassessed the role of DFI in the model. In doing so, we have considered classical measures for model spinup activity, such as the domain-averaged absolute tendency of the model fields, the root-mean square of the model field tendencies, or time series of model fields at specific gridpoint locations. The latter have appeared to be the most informative diagnostics for our concern, since they provide local information that can give insight into some temporal or spatial aspect of a signal (as will be shown below). Figures 1 and 2 show time series of mean sea level pressure (MSLP) for the five sensitivity experiments listed in Table 1, measured for a model grid point located in the inner core of the ALADIN-France domain and over the sea (here, the Bay of Biscay) for Fig. 1 and a grid point positioned inside the Davies relaxation zone (Fig. 2). The goal here is to assess the traces of inertia–gravity waves, by means of the differences of the various sensitivity runs with respect to a, presumably noise-free, reference. The reference run is EX1, which is an ALADIN forecast started using as its initial conditions a 6-h forecast. As for all five runs, no DFI is applied in EX1. From Fig. 1, it is clear that the time evolution of MSLP is rather smooth. There is no graphical evidence of spinup in this restart experiment, despite the fact that we do not provide all $t - dt$ fields, nor the physics tendencies for the restart time t. Note furthermore that in EX1, we use ''old'' lateral boundary conditions (LBCs) so that the core and LBC fields do match at the initial time in the relaxation zone. In EX2, we change both the initial conditions (to a 3DVAR analysis) and the LBC data (to LBC obtained from the up-to-date ARPEGE run, which is also denoted as ''refreshed'' LBC). If DFI was set on, this configuration would be the equivalent of an operational ALADIN-France forecast. In EX2, however, DFI is switched off and one notices the existence of a wavy, rather nonperiodic, pattern on MSLP right from the start of the integration. A fairly parallel MSLP time curve in EX2, compared with EX1, is obtained after about 30 model time steps (about 3.5 h). Thus, the first

TABLE 1. Summary of the five sensitivity experiments performed to track gravity waves due to patterns of initial spinup behavior. None of the experiments uses DFI. In the description of the experiments, *H* stands for the initial time (or network) of the experimental run and $H - 6$ h refers to the previous network time 6 h earlier. Thus, the $H - 6$ h global run data correspond to the ARPEGE model data obtained from the network time prior to the initial time of the experiments (having a 6-h cycling sequence in mind). The *H* global run data are ARPEGE data from the same network time than the initial time.

Expt	Initial conditions	Lateral boundary conditions	Comments
EX1	First guess (6-h forecast)	Interpolated from the $H - 6$ h global run (''old'' coupling data)	Quite close to a warm start
EX2	3DVAR analysis	Interpolated from the *H* global run (''fresh'' coupling data)	Data similar to the operational assimilation (except no DFI)
EX3	First guess	Interpolated from the *H* global run	Run to assess the impacts of mixed data in the relaxation zone
EX4	3DVAR analysis	Interpolated from the $H - 6$ h global run	Mixed data also in the relaxation zone but in a complementary way to EX3
EX5	3DVAR analysis	0-h coupling file is the analysis, subsequent 3-hourly files are similar to EX1 and EX4	Run to assess the impacts of imposing spatially consistent data in the relaxation zone at the initial time

information in EX2 is that a forecast started from an ALADIN 3DVAR analysis, along with refreshed coupling data from ARPEGE, does possess wavy structures that are not present in a ''restart'' experiment. This result has also been obtained for several other cases, which shows that these patterns are not just the signature of a meteorological feature that would have been captured by the data analysis process in the particular situation displayed in our graphics. This type of feature corresponds to a pattern of spinup behavior. Operational experience furthermore tells us that these wavy patterns are not seen when DFI is switched on. With DFI and the tunings discussed in section 1, time series of model outputs exhibit a smooth evolution both in their dynamical adaptation and in data assimilation mode.

Another question of interest is to what extent the analysis increment does introduce such wavy, unbalanced, behavior. From other ALADIN studies, especially in relation to so-called blending cycles (e.g., Brožkovà et al. 2001; Širokà et al. 2001), we know that the choice of the LBC data can have an impact on short-term forecast performances and spinup properties. Thus, we have run experiment EX3, which is started from the same initial fields as EX1 but which uses the refreshed LBCs, like EX2. Conversely, we have run an experiment (EX4) that is started from the 3DVAR analysis like EX2, but that uses the same LBCs as in EX1. In Fig. 1 and for EX3, we notice a very clear periodic pattern associated with a wave in MSLP passing over the point in the Bay of Biscay after about seven model time steps. This pattern disappears only after about 30 model time steps, which is slightly beyond the first LBC update time (3 h) in the forecast, since we use a 3-h coupling frequency. The MSLP curve for EX4 first follows the evolution of EX2, until about six or seven time steps, and then becomes dominated by a very periodic wave signal that lasts for about the same duration as in EX3.

Let us now compare the MSLP time series over the Bay of Biscay with the time series for MSLP at a point in the relaxation zone. At the latter location, the model forecast fields will be partially controlled by the coupling model solution. Referring now to Fig. 2, we see a smooth MSLP evolution for EX1, a rather periodic wavy curve for EX2 and EX3 (for about 20–30 time steps and, here, starting right from the beginning of the simulation), and a fairly nonperiodic wavy pattern for EX4 (over about 30 time steps). Thus, similar oscillations are observed at both points, in the relaxation zone and in the interior domain (Bay of Biscay).

Not shown in this paper are the spatial structures of the wavy patterns, as obtained by simply plotting the difference of MSLP between any sensitivity experiment and the reference EX1, which we have done for every 1-h time step. From these plots, we have inferred that the nonperiodic wavy feature obtained for EX2 mostly corresponds to a spatially unstructured field in which no specific horizontal patterns are visible. We interpret the unstructured nature of the MSLP difference maps as being a signature of a complex reequilibration of the analysis in the model spinup phase. Thus, one may consider the hills and valleys for EX2 in Fig. 1 as a signal of the imbalance in the analysis increment. This imbalance generates MSLP variations of about 0.7–0.8 hPa. With regard to EX3 and EX4, the spatial maps of the MSLP forecast differences have shown a fairly structured wavy pattern, though they do not correspond to a pure sinusoidal signal (rather a succession of pluses and minuses in the field, with irregular but smooth contours). Furthermore, we found graphical evidence that the wavy pattern is generated at an inflow boundary of the model domain and very quickly propagates inward. From the plots, and from the time of appearance of the periodic signal on the MSLP time series of EX3 at the two points displayed in Figs. 1 and 2, the speed of the propagation

of the corresponding wave is estimated to be about 1200 km h^{-1}. This speed would correspond to the phase velocity of the external inertia–gravity wave for a uniform-density fluid with an equivalent height of about 11 km. The wave graphically appears as a broad (spatial pseudo-wavelength of about 450 km) and deep structure, which is the result of the imbalance within the relaxation zone, and it is sufficient to simply use spatially mismatching fields to produce it. Indeed, in EX3, the wavy pattern is created despite the balanced initial state in the core of the domain. However, the linear combination of that forecast state with the refreshed LBC data used in the Davies formulation is not balanced. A similar problem affects EX4, which also has mismatching lateral boundary and inner domain fields. We further notice that the periodic signals seen in Figs. 1 and 2 are reminiscent of signals obtained, for instance, in noninitialized High Resolution Limited Area Model (HIRLAM) forecasts [see Fig. 6 in Lynch and Huang (1992)].

Previous experimental studies within the ALADIN community, for various types of 3DVAR assimilation cycles, have indicated that spatially consistent (matching) data for the inner domain and the LBC initial fields can reduce the size of the digital filter increment around the lateral boundaries (Širokà et al. 2001). Thus, in order to verify whether a rather straightforward spatial match of core and boundary initial data would be sufficient to reduce the boundary-generated spinup, we have run experiment EX5, where the 3DVAR analysis is used both for the initial inner domain and LBC data. It turns out that EX5 also exhibits wavy structures on the MSLP curves, and that they are about as pronounced as in EX4. In Figs. 1 and 2, the differences between EX1 and EX3 are striking, while the patterns of behavior of EX4 and EX5 remain fairly similar. This graphical evidence suggests that the model balance for the LBC data probably would be even more beneficial than the mere spatial consistency. As an intermediate conclusion, we exhibited two different sources of spinup: one linked with the 3DVAR analysis increment and the other linked with the imperfect match of interior and lateral boundary conditions at initial time.

b. *Consequences of the use of digital filters*

From the findings summarized in section 2a, we have run alternative assimilation configurations, changing the choices for the initial LBC data (spatially matching or not) and the settings for the digital filtering. Namely, we have tested reducing the filter's time span and stop-band edge period. Keeping in mind that ''boundary waves'' might appear occasionally, with time periods between 0.75 and 1.5 h (see Figs. 1 and 2), we have reduced the stop-band edge τ_s from 3 to 2 h but not less. At the same time, the time span also can be slightly reduced from about 2 to 1.6 h setting $N = 9$ down to $N = 7$ (N as defined in the appendix). The latter change keeps the response function nearly untouched (similar ripple ratio) while diminishing slightly the numerical cost of the DFI. As concerns the analysis increment oscillations, it is difficult to spot a clear time period associated with them. The new settings proved experimentally to be valid choices for removing these analysis-related signals. In the MSLP time series for EX2 and EX5, one for instance cannot notice any significant oscillatory signal with a period longer than 2 h.

A further change of interest for the ALADIN LAM assimilation was the switch from nonincremental filtering, where forecasts are started with $f(a)$, to incremental filtering, where forecasts are started with $g + f(a) - f(g)$ (g standing for the first guess). Initialization using the incremental formulation and digital filters is denoted here as IDFI. The effective ''total increment'' for nonincremental filtering is $f(a) - g$, with both an impact coming from corrections by the observations and the 3DVAR background error covariances, and an effect due to the application of the digital filter. We have found on several occasions that the two signals tend to overlap, especially in meteorologically active areas such as frontal structures, where one still would wish the analysis to remain the dominating process of ''correction of the first guess.'' Rewriting $f(a) - g = f(a) - f(g) - [g - f(g)]$ shows that the (nonincremental filter) total increment amounts to adding to the first guess the balanced analysis increment, but also to removing the filtered part of the first guess. This is not a problem if the first guess itself is in balance in the sense of the filter f, since then $g - f(g)$ vanishes. However, if we come back to digital filtering, f behaves by definition as a temporal filter and the term $g - f(g)$ is nonzero if one admits that high frequencies can exist in g in relation to rapidly evolving meteorological features, for instance. Consequently, the high frequencies present in the first-guess field will be removed from the initial state in the nonincremental case, although one would hypothesize that these ''oscillations'' are not of the spinup type. Moreover, the total increment $f(a) - g$ may depart significantly from the optimum in terms of assimilation theory, an aspect that is in principle true regardless of whether DFI or IDFI are used. Conversely, with incremental filtering, the high frequencies in g are kept in the initial state for the subsequent forecast.

The use of incremental filtering for initialization in an assimilation cycle has been promoted in various works in the past. Puri et al. (1982) compared incremental linear normal mode initialization with Machenhauer's NNMI in a hemispheric nine-level primitive equations

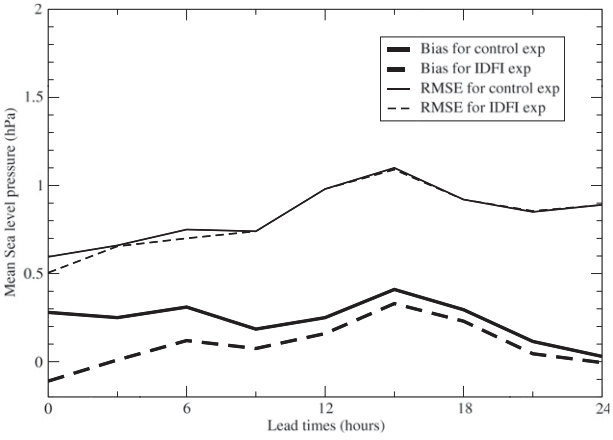

FIG. 3. Scores of biases (thick curves) and RMSEs (thin curves) of MSLP with respect to the French surface station network, for the operational ALADIN-France model (nonincremental DFI, solid lines) and for the test model (incremental DFI, dashed lines). Units are model lead times from 0 to 24 h, every 3 h (horizontal axis), and hPa (vertical axis). Note that lead time 0 corresponds to the initialized analysis.

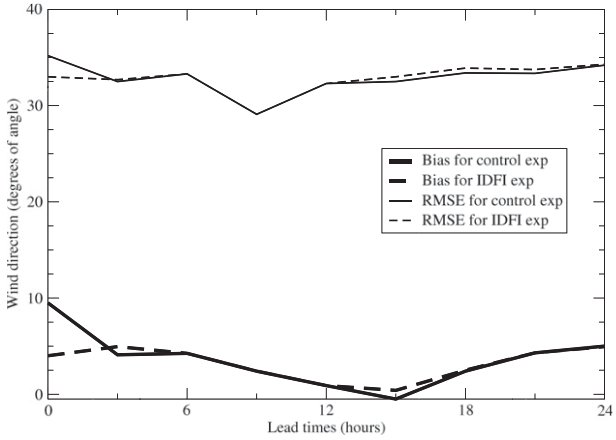

FIG. 4. Scores of biases (thick curves) and RMSEs (thin curves) of the direction of the 10-m wind vector with respect to the French surface station network, for the operational ALADIN-France model (nonincremental DFI, solid lines) and for the test model (incremental DFI, dashed lines). Units are model lead times from 0 to 24 h, every 3 h (horizontal axis), and degrees (vertical axis). Note that lead time 0 corresponds to the initialized analysis.

model. They showed that the incremental linear version was able to filter gravity wave noise from the analysis while keeping a strong signal of the mean meridional circulation, especially in the model's tropics. They also noticed some residual transient gravity wave activity, a finding that they presumed to be harmless. Ballish et al. (1992) proposed an alternative method, leaving the context of a linearized initialization and transposing the incremental approach to NNMI. Using the global National Meteorological Center [NMC, now known as the National Centers for Environmental Prediction (NCEP)] model, they applied the NNMI code to the difference of the model tendencies starting with the analysis and the first guess, respectively. The result is added back to the analysis, and a final initialization step follows before the forecast. They claimed that this approach is less sensitive to the way diabatic tendencies are computed, as the potential uncertainties in the model physics, which could lead to incorrect gravity wave removal in NNMI, are partially canceled by the subtraction step. Their results show that the incremental method keeps the signal of tidal waves, especially the semidiurnal wave in their settings, much more untouched than does the nonincremental NNMI. They also show that the incremental NNMI produces a better balanced state within the assimilation cycle than Puri et al.'s linear incremental version, by removing more efficiently transient waves. The benefit, in terms of balances, of incremental initialization has been then further confirmed within the context of 3DVAR global assimilation systems (see, e.g., Courtier et al. 1998). In four-dimensional variational data assimilation (4DVAR) Gauthier and Thépaut (2001) have introduced an incremental filtering formulation directly inside the data assimilation process, by adding a weak-constraint cost function based on digital filters (the so-called Jc-DFI term in 4DVAR, one variant of the J_c term introduced in section 1). This approach allows one to filter the analysis increment while performing the data assimilation step, at a very marginal extra numerical cost. Despite its intrinsic linear formulation, this filtering should control nonmeteorological transient waves thanks to the presence of the observational constraint.

The quantitative effects on objective scores when switching from the operational, nonincremental, DFI toward retuned IDFI are shown in Figs. 3–5 for MSLP, and 10-m wind direction and wind speed, respectively. We display both error bias and root-mean-square error (RMSE). As an important point here, note that while surface pressure is assimilated in the ALADIN-France 3DVAR, 10-m wind observations are not assimilated in the operational version discussed in this section 2. Accordingly, in our companion experiment using IDFI, 10-m wind observations are not included, and can be considered to be genuine cross-validating data throughout section 2. The scores are obtained with respect to the French mesoscale surface network, for a period of 40 days (20 September–31 October 2006). A further difference, namely the overall tuning of the ratio between background and observation error variances [setting R from 1.5 to 1.2; see Fischer et al. (2005, p. 3481)], is an additional change entering this comparison. This retuning however does not have a significant impact on the statistical scores displayed in this section. The major impact of IDFI is a decrease on the MSLP error bias, with also

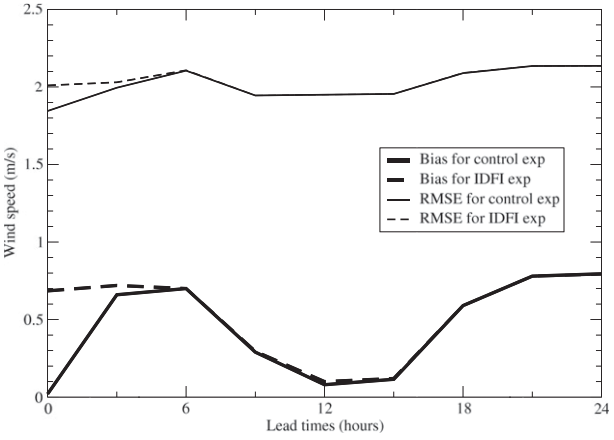

FIG. 5. Scores of biases (thick curves) and RMSEs (thin curves) of the 10-m wind speed with respect to the French surface station network, for the operational ALADIN-France model (nonincremental DFI, solid lines) and for the test model (incremental DFI, dashed lines). Units are model lead times from 0 to 24 h, every 3 h (horizontal axis), and m s^{-1} (vertical axis). Note that lead time 0 corresponds to the initialized analysis.

a fairly small reduction of the RMSE in the short-term forecasts, mostly felt until 6-h lead time (Fig. 3). Note that, at other time periods when the operational MSLP error bias was negative, IDFI further decreased the bias, thus leading to a slightly more negative bias with respect to the observations. Therefore, this effect of IDFI, tending to decrease the MSLP bias, cannot systematically be considered to be an improvement. We rather interpret this signal as an effect of the intrinsically biased nature of the nonincremental formulation of the digital filter (see the appendix). For the 10-m wind *direction*, the most prominent impact is a much better fit of the 3DVAR + IDFI initial state with respect to the observations, compared with the operational version (Fig. 4). This finding is in accordance with subjective verification, which indicated that the large-scale 10-m wind orientation is more consistent with MSLP structures (gradients) in the IDFI-derived initial model state. An apparent ''drawback'' of IDFI is the deterioration of the initial and 3-h lead-time 10-m wind *speed* bias and RMSE (Fig. 5). Thus, IDFI does have opposed effects on the wind field, in terms of scores to observations: a positive impact is obtained for the 10-m wind direction, and a negative one is seen on the 10-m wind intensity.

To be more specific, the overestimation of low-level wind speed, most notably during night, is known as a typical shortcoming of the ALADIN model version used in our study. This overestimation was seen in routine experiments of that time both in ARPEGE and ALADIN, and for any forecast lead time corresponding to nighttime conditions (F. Bouyssel 2009, personal communication). Within the framework of our discussion, this aspect will be considered to be a typical model error term whose investigation is beyond the scope of our work. To understand more in depth, however, the link between this overestimation of wind intensity and the strategy for filtering the initial state, we have run two extra experiments. Both experiments consist of series of forecasts over the full 40-day period, started respectively from archived nonfiltered 3DVAR analyses (initial state is a) and archived (nonincrementally) filtered first guesses [initial state is $f(g)$]. The archived data originate from the operational ALADIN-France 3DVAR and no assimilation cycle was run for these two extra experiments. The 10-m wind speed scores for the experiment started from nonfiltered analyses superpose almost perfectly with those of the IDFI assimilation experiment. The scores of the $f(g)$ experiment reveal a drop of the bias almost to 0 and a slight decrease of the RMSE, exactly as for the operational assimilation using nonincremental DFI. Thus, it is DFI that brings the initial states closer to the observations of 10-m wind speed, and not the 3DVAR analysis. Nonincremental DFI impacts on the 10-m wind field, regardless of which term is the input state (an analysis a or a forecast g), in a way leading to a better fit toward the observations. This positive impact is however lost after about 3 h of integration. In the IDFI assimilation, as well as in the series of forecasts started from nonfiltered analyses, the low-level wind speed differences between the observations and model initial states are relatively close to the differences between the observations and 6-h forecasts (the backgrounds to the analyses). Eventually, the wind speed error bias and RMSE will tend to approach values representative of forecast errors.

We also checked the two extra series of 40-day forecasts, started from a and $f(g)$, with respect to MSLP and 10-m wind direction scores. The scores of the forecasts that were started from nonfiltered analyses were roughly similar to those of the IDFI assimilation experiment, especially as concerns MSLP and 10-m wind direction biases over the 40 days. The scores of the forecasts started from filtered first guesses revealed increased MSLP bias and RMSE, as well as a clearly increased 10-m wind direction bias at 0 h, with respect to the IDFI assimilation. Actually, the scores for the $f(g)$ experiment were close to those of the operational assimilation with nonincremental DFI [remember that the $f(g)$ experiment is not cycled, so that model errors cannot diverge to large ''climatological'' values]. Thus, the application of the nonincremental DFI systematically leads to an increase of the MSLP bias along with a slight increase in MSLP RMSE. Conversely, application of no or incremental DFI results in a systematic drop in the MSLP error bias, compared with the nonincremental DFI. In terms of low-level wind direction, subjective verification reveals that low-level wind vectors

tend to be more consistent with the isobaric contours in the IDFI case.

Among all aspects, formulation of the filter, tuning of the filter parameters, and tuning of the weighting factor R in the range [1.2, 1.8] (see Fischer et al. 2005), the most prominent impact came from changing the digital filter formulation from nonincremental to incremental. The retuning of the time span and stop-band edge period did have a second-order impact in terms of scores. Other aspects noticed during the comparison of nonincremental DFI versus IDFI were the systematic signal of a drop in the scores of the MSLP bias and the more significant similarity between the total IDFI increments and 3DVAR analysis increments than with simple DFI. As a consequence of the accumulated experience from Fischer et al. (2005) and the present study, we have decided to introduce IDFI inside the ALADIN-France 3DVAR assimilation cycle and forecast production process, accepting the deterioration of the low-level wind speed score in the 0–3-h model states, and the drop observed in the MSLP bias. The previous experiments and results were obtained without assimilating some of the verifying data, namely the 10-m wind observations from the surface synoptic observation (SYNOP) and French mesoscale surface networks. In section 3, we illustrate the impacts of adding the 10-m wind observations into the 3DVAR assimilation.

3. Additional low-level wind information in the analysis

We now investigate the impacts of the IDFI formulation on data assimilation, that is to say, how IDFI can modify the relative signal in an observation sensitivity experiment (OSE) framework. We test the differential impacts of 10-m winds in OSEs using either incremental or nonincremental DFI. As we will show in this section, the impacts of 10-m wind assimilation affect forecast fields that are otherwise also impacted by the choice of the filtering option. This experimental finding has motivated our discussion in this section. Conversely, please note that the assimilation of 10-m winds will not address some shortcomings in the model's performance described in section 2b. To be specific, our intention is not to correct the negative impacts of the changes to IDFI in the scores of 10-m wind speed, by assimilating 10-m wind observations. This negative aspect has to be addressed by improvements in the prognostic model. In this section, we address the complex interpretation of OSEs with respect to other aspects of the assimilation system design, here initialization.

The 10-m wind observations (also referred as screen-level winds) are very common data. However, their use inside data assimilation systems is more unusual. There are several reasons for this; the model equivalent for these observations is of poor quality, because 10-m winds strongly depend on surface parameters (orography, roughness length) that are small-scale data that vary greatly inside a typical grid mesh of the model. In other words, 10-m wind observations give local information. Another problem for their assimilation is the fact that these observations are mainly representative of planetary boundary layer (PBL) processes. Thus, depending on the vertical resolution of the model, care needs to be taken as concerns the vertical propagation of the information brought by these observations into the analysis: the 10-m level might not be representative of a higher part of the PBL, and the further vertical propagation of the associated signal into the free troposphere can be even more detrimental. This aspect is of particular importance under stable conditions. On the other hand, screen-level data might contain valuable information about the low-level convergence field and, thus, have a positive impact on the forecast of frontal or convective situations.

Thus, the usage of these observations might be inappropriate for large-scale models. On the contrary, a small-scale assimilation system could benefit from these data, for instance, because it would have specific background error covariances. Shorter-scale background error correlation length scales will induce smaller-scale analysis increments, or equivalently a shorter propagation of information associated with a local piece of observation. This aspect of a regional assimilation system has for example been observed when comparing typical background error covariances sampled either from a large-scale coupling system (ARPEGE) or from the coupled LAM system [in the case of ALADIN-Morocco, see in Sadiki et al. (2000), or for ALADIN-France, see in Ştefănescu et al. (2006)]. Additionally, a higher-resolution model presumably should better represent local fields, simply through the systematic adaptation of the forecast fields (and, thus, the background fields) to the surface forcings.

Within the context of the ALADIN-France model, a preliminary work for 10-m wind assimilation was to make a selection of stations that are in good agreement with our model, that is to say, locations where the difference between the model and reality (e.g., in terms of orography) is weak. As discussed above, our goal is to retain only observations that are representative of the model equivalent. As a result of this elimination stage, about 2000 pieces of individual data are provided to our ALADIN-France 3DVAR assimilation system. The experiments were run over a period of 45 consecutive days starting on 1 March 2008. They all consist of a 3DVAR assimilation cycle with a 6-h frequency, and include a production forecast once a day at 0000 UTC. Results of four different experiments

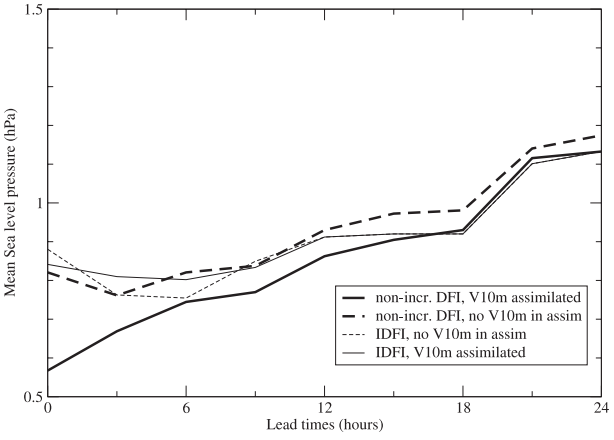

FIG. 6. RMS of the differences between experiment and observations for MSLP, computed every 3 h (see graphics legend for details about the experiments).

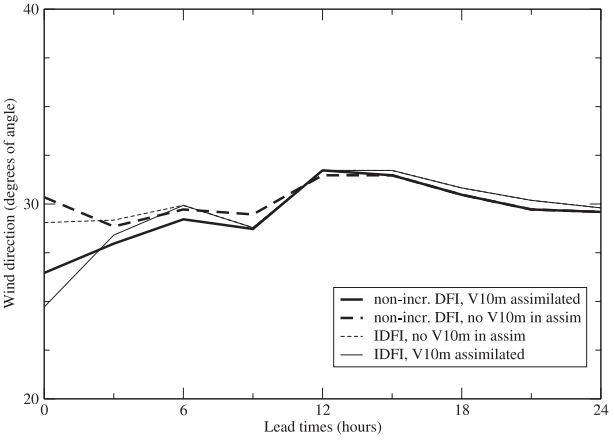

FIG. 7. RMS of differences between experiment and observations for 10-m wind directions, computed every 3 h (see graphics legend for details about the experiments).

are presented: filtering with DFI and no 10-m winds assimilated, DFI plus 10-m winds assimilated, IDFI filtering with no 10-m winds in the assimilation, and IDFI plus 10-m winds in the assimilation.

A first apparent impact of assimilating 10-m winds with DFI is an improvement in the RMSE for MSLP, possibly up to 18 h ahead (see the two thick curves in Fig. 6). Beyond 18 h, the impact becomes much less marked and difficult to analyze. According to a simple statistical test, the differences are nonsignificant past 12 h. If now, one compares the DFI versus IDFI curves, one notices that, for this test period, the RMSE is slightly bigger for IDFI than for DFI at the initial time, and only slightly lower for the 6-h range (cf. the two dashed curves). The effects of the net decrease of the MSLP bias with IDFI are also again observed, and they are very similar to those displayed in Fig. 3 and discussed in section 2b (thus, the bias curves are not shown for the OSEs in this section). The impact of the assimilation of 10-m winds in the IDFI case however appears very unclear. On the whole, the effects seem positive at the initial time, and slightly negative, for instance, for the 3- and 6-h ranges. Eventually, one is unable, in the IDFI case, to derive any firm conclusions on the impacts of 10-m winds considering only the RMSE score of the MSLP. We further notice that the positive signal induced by the 10-m winds is of fairly small amplitude, and of quite similar magnitude, when compared to the impacts due to the choice for the filtering. Indeed, the changes to the biases and RMSEs of MSLP observed in any of our experiments are of about a few tenths of a hectopascal (Figs. 3 and 6). Therefore, the conclusions of the OSE study actually would differ, if MSLP were the sole field of concern and only one precise version of the assimilation system would be evaluated (DFI or IDFI). In terms of spatial structure or dynamical balances, it also appeared to us to be fairly delicate to understand the possible interactions between our filtering strategy and the assimilation of 10-m winds. Assimilating the 10-m winds may help us reduce the errors in the mass field at the mesoscale, but the analyzed state can then contain some level of imbalance because the observations also would be to some extent representative of very local aspects not represented in the model (e.g., orography unseen on the model grid, despite the data selection discussed above).

With regard to the screen-level wind direction, there is an impact in terms of proximity to the 10-m wind observations, as displayed in Fig. 7 (see the two thick curves for the DFI case): the initial state with 10-m winds indeed has a closer fit to these data than when 10-m winds are kept out of the assimilation process. A similar impact can be seen on 10-m wind speed (not shown). This closer fit still is observed for the 3-h lead time, and then disappears for 6 h and beyond. A similar impact, though less pronounced in time, is retrieved when an IDFI filtering strategy is retained (cf. the two thin curves in Fig. 7 now). A simple statistical test on the differences of RMSE confirms that the impacts of assimilating 10-m winds on 10-m wind RMSEs is only significant for the 0- and 3-h ranges, in both the DFI and IDFI cases. For longer forecast ranges, model errors for 10-m winds rapidly overcome the gain in terms of wind initialization (we refer to our discussion in section 2b).

As a conclusion to this section, the impacts of 10-m winds in the assimilation system are, as expected, to bring the initial state and the very short-term forecasts closer to the 10-m wind observations. The impacts are, however, fairly unclear when MSLP is considered, with any tentative conclusion depending on the assimilation system design. The latter finding points to some general

criticisms raised against applying any filtering inside a data assimilation procedure. Indeed, any filter will, to some extent, wipe out part of the fit to the observations or more generally the statistical properties of the unfiltered analysis.

4. Conclusions

In section 2a, we have presented examples of inertia–gravity waves resulting from initial state imbalances: some are caused by the analysis increment, others are due to lateral boundary condition mismatches. For the latter waves, an appropriate choice of spatially consistent boundary fields, and, possibly, the specifications of balanced lateral boundary conditions, can reduce the pattern of spinup behavior. Considering the ALADIN-France regional forecast model, we have derived from these findings tuned parameters for a digital filtering initialization. Furthermore, we have discussed and tested an incremental formulation of the digital filter. We refer the reader to section 2b for a historical overview of the uses of incremental strategies for initial state filtering in NWP. The two most noticeable impacts of moving from a nonincremental to an incremental DFI in the ALADIN-France system were found to be the following:

- A net decrease of the mean sea level pressure bias (with respect to observations) was shown. This systematic difference of MSLP bias is at least partially linked with the intrinsic biased formulation of our DFI. Indeed, the filtering procedure consists of a succession of adiabatic and diabatic model integrations, a situation that is known to introduce a bias between the filtered state and the original state (see the appendix).
- Some significant modifications to the short-term scores with respect to observations were discovered. In particular, short-term scores with respect to 10-m wind observations were modified, with IDFI having a positive impact on the score for wind direction but a negative one for wind intensity. The former impact resulted in wind vectors being subjectively more consistent with the MSLP field, while the latter impact eventually was accepted as a ''necessary'' drawback when switching to IDFI.

In section 3, we discussed the impacts of DFI and IDFI on the results and evaluations of OSE studies. We used the additional assimilation of 10-m wind observations from the French high-density surface network as an example. The results mostly show a similar effect on the scores of the extra assimilated field itself, namely a reduction in the 10-m wind RMSEs in both the DFI and IDFI versions of the assimilation system. These results are consistent with basic data assimilation expectations. For MSLP, however, the evaluation of the OSE results remains very open, with an apparent positive impact in the nonincremental DFI case, and no clear signal at all with IDFI. This finding points to the sometimes delicate interpretation of scores in OSEs, when the impacts from observations are of fairly small amplitude and may be comparable to the impacts of some other modifications in the assimilation system. One might consider that the positive impacts of assimilating 10-m winds with the nonincremental filtering formulation, mostly visible on MSLP RMSE, should be an incentive to combine the simple DFI with the assimilation of 10-m winds. However, we then would obtain again other drawbacks with nonincremental DFI, like the MSLP bias signal and the filtering of rapidly evolving features present in the first guess (and presumably of valuable interest). Adopting an opposite view, removing any type of filtering would totally eliminate spurious interactions of the initialization step with OSE sensitivities. However, as discussed above, such removal is not suitable since it opens the door to various types of spinup behavior patterns that will in turn hamper the evaluation of the OSE experimentation. Eventually, while we decided to stick to the choice of IDFI in the ALADIN-France 3DVAR, we would not claim that the present study is a benchmark proof that IDFI is superior to DFI in any experimental context. We do claim that some filtering is needed in our system, and that it can in turn alter the interpretation of OSE studies when the sensitivities are fairly small.

For the longer-term perspectives, several issues can be considered. Alternative lateral boundary condition formulations, compared with Davies relaxation, might lead to very different patterns of behavior along the lateral borders of the LAM. With the forecast model design of the ALADIN-France type in mind, some work already has been undertaken within a simplified framework [e.g., Termonia and Voitus (2008); Voitus et al. (2009), which have shown the fair difficulty of developing and ''outperforming'' Davies relaxation]. As discussed earlier, some spinup waves possibly could be removed or decreased by specifying balanced LBC fields. The exact, detailed characteristics of spinup waves also depend on the overall model specifications and properties. Changes in model dynamics (advection scheme, diffusion, bottom- or top-boundary conditions) or physics may alter the amplitude and propagation of inertia–gravity waves. Therefore, within the context of either a research or an operational model, we advise a regular check of the spinup properties using some basic experimental settings in the spirit of our study (e.g., computing a reference, presumably a spinup-free forecast, from a previously forecast state with which to compare any sensitivity experiment). Changes in the model also may affect the interpretation of model scores,

since model errors may have changed. For these studies, we stress the usefulness to carefully identifying and describing existing spinup waves so as to optimally tune the filter parameters.

In the specific case of a cycled data assimilation system, the fact that the background state for the analysis is a previous forecast should possibly allow for no or very little filtering. This conjecture does not, to this point, hold in the ALADIN-France 3DVAR. In a 4DVAR system, the removal of DFI or IDFI, while possibly using a DFI-formulated penalty function inside the minimization problem (Jc-DFI), may lead to a non- or only weakly filtered system.

In dynamical adaptation mode (see section 1), our experience with various versions of the ALADIN model indicates that some filtering is mandatory. Filtering then is of the nonincremental DFI type. One reason for this need is the imbalances of the interpolated fields when going from the coupling to the coupled model grid. As long as the resulting spinup problems appear as fairly well-defined waves in the temporal spectrum, with a concentration in the high frequencies, properly tuned DFI will almost completely remove these waves. However, by doing so, DFI also would remove possible high-frequency meteorological signals and, thus, potentially deteriorate the short-term forecast on those aspects. Termonia (2008) has analyzed this problem by identifying fast propagating signals with a Doppler effect and introduced a scale-selective DFI that filters some high frequencies while preserving large-scale rapid modes. To achieve this modified behavior, Termonia formulates DFI in space–time frequency space, and the cutoff parameter is defined as a phase speed (as opposed to a time frequency in the classical digital filter). This scale-selective formulation is not specific to the dynamical adaptation context and may be applied and tested in a data assimilation system.

Acknowledgments. First of all, we thank Dominique Giard for her long-standing efforts on designing and promoting initialization techniques within the ARPEGE and ALADIN communities. The technicalities provided in the appendix go back to Giard's lecture course on DFI. We are also grateful to the three reviewers of the manuscript, who helped improve the discussions in our paper.

APPENDIX

Usual Formulation of the Nonrecursive Digital Filter within an ALADIN Context

The problem with initialization is in providing the numerical forecast model with a filtered state, valid at the initial time and expressed in terms of model prognostic fields and discretization grid. Within the context of numerical filtering, we then look for nonrecursive filters that require both past and future model states:

$$\bar{x}_0 = \sum_{n=-N}^{+N} h_n x_n, \tag{A1}$$

where n stands for any model time step, N is the total span of the filter (expressed in model time steps), and x_n is any model state (and one time step propagates the model solution from x_n to x_{n+1}, for instance). Note that the digital filter formulation is expressed here as a convolution with time, and thus it is equivalent to a simple multiplication of the time Fourier transform of the model solution X by the response function of the filter H: $H(\omega) \times X(\omega)$, where ω stands for frequency.

Digital filters in ALADIN have been introduced following Lynch (1997) and Lynch et al. (1997). The usual choice then is the Dolph-Chebyshev filter:

$$H(\omega) = T_{2N}\left[\frac{\cos\left(\frac{\omega\Delta t}{2}\right)}{\cos\left(\frac{\omega_s\Delta t}{2}\right)}\right] \Bigg/ T_{2N}\left[\frac{1}{\cos\left(\frac{\omega_s\Delta t}{2}\right)}\right], \tag{A2}$$

where $T_n(\cdot)$ is the Chebyshev polynomial of order n, Δt is the time step, $\omega_s = 2\pi/\tau_s$ with τ_s standing for the stop-band edge period of the filter, $\omega = 2\pi/t$, and t is time. In practice, the following guidelines have been retained for applications in ALADIN (Lynch et al. 1997):

- Within the stop-band edge period $[0, \tau_s]$, the response function has a maximum deviation from zero of about $r = 0.14$ for $\tau_s = 3$ h and a filter time span of $T = 2N\Delta t = 2.5$ h. The efficiency of the filter is increased when the time span is increased, for instance, $r = 0.01$ when $T = 5$ h. The term ripple ratio is also used for r.
- The efficiency of the filter can also be increased by applying the filter several times. For two successive filterings, $r = 0.02$, keeping $T = 2.5$ h. A drawback here is that frequencies lower than but close to ω_s also will be more filtered when applying the filter twice than when used only once.
- In order to obtain a filtered state that will remain "close" to the original analysis (to be filtered), the above filter is applied twice in the following sequence: first, run the adiabatic model "backward" in time from $t = 0$ to $t = -2T$, and apply the filter while integrating. An adiabatically filtered state is thus obtained for $t = -T$. From this state, run the full (including physics) model forward in time until $t = +T$ and filter while integrating. The final result is a doubly filtered state valid at $t = 0$.

- The cost of the digital filter is about the cost of one adiabatic $2T$ forecast, plus one full model $2T$ forecast. This cost might be nonnegligible for a very high-resolution model, using sophisticated microphysics for instance.
- The fact that the backward integration involves the adiabatic model (with only numerical horizontal diffusion turned on) implies that a *bias is generated in the final filtered state, with respect to the original analysis state.*

REFERENCES

Ballish, B., X. Cao, E. Kalnay, and M. Kanamitsu, 1992: Incremental nonlinear normal mode initialization. *Mon. Wea. Rev.,* **120,** 1723–1734.

Berre, L., 2000: Estimation of synoptic and mesoscale forecast error covariances in a limited area model. *Mon. Wea. Rev.,* **128,** 644–667.

Brožkovà, R., and Coauthors, 2001: DFI blending: An alternative tool for preparation of the initial conditions for LAM. Research activities in atmospheric and oceanic modelling, WMO CAS/JSC WGNE Rep. 31, 1.7–1.8.

Courtier, P., C. Freydier, J.-F. Geleyn, F. Rabier, and M. Rochas, 1991: The ARPEGE project at Météo-France. *Proc. 1991 ECMWF Seminar on Numerical Weather Prediction Methods,* Reading, United Kingdom, ECMWF, 193–231.

——, and Coauthors, 1998: The ECMWF implementation of three-dimensional variational assimilation (3D-VAR). I: Formulation. *Quart. J. Roy. Meteor. Soc.,* **124,** 1783–1807.

Davies, H., 1976: A lateral boundary formulation for multi-level prediction models. *Quart. J. Roy. Meteor. Soc.,* **102,** 405–418.

Derber, J., and F. Bouttier, 1999: A reformulation of the background error covariance in the ECMWF Global Data Assimilation System. *Tellus,* **51A,** 195–221.

Fischer, C., T. Montmerle, L. Berre, L. Auger, and S. Ştefănescu, 2005: An overview of the variational assimilation in the ALADIN/France numerical weather-prediction system. *Quart. J. Roy. Meteor. Soc.,* **131,** 3477–3492.

Gauthier, P., and J.-N. Thépaut, 2001: Impact of the digital filter as a weak constraint in the preoperational 4DVAR assimilation system of Météo-France. *Mon. Wea. Rev.,* **129,** 2089–2102.

Geleyn, J.-F., and Coauthors, 1995: Atmospheric parametrization schemes in Météo-France's ARPEGE N.W.P. model. *Proc. Seminar on Physical Parametrizations in Numerical Models,* Reading, United Kingdom, ECMWF, 385–400.

Haugen, J., and B. Machenhauer, 1993: A spectral limited-area model formulation with time-dependent boundary conditions applied to the shallow-water equations. *Mon. Wea. Rev.,* **121,** 2618–2630.

Horányi, A., S. Kertész, L. Kullmann, and G. Radnóti, 2006: The ARPEGE/ALADIN mesoscale numerical modeling system and its application at the Hungarian Meteorological Service. *Idöjárás,* **110,** 203–227.

Huang, X.-Y., and P. Lynch, 1993: Diabatic digital filter initialization: Application to the HIRLAM model. *Mon. Wea. Rev.,* **121,** 589–603.

Lynch, P., 1990: Initialization using a digital filter. *Research Activities in Atmospheric and Oceanic Modeling,* H. Ritchie, Ed., CAS/JSC WGNE Rep. 14, WMO, 1.5–1.6.

——, 1997: The Dolph–Chebyshev window: A simple optimal filter. *Mon. Wea. Rev.,* **125,** 655–660.

——, and X.-Y. Huang, 1992: Initialization of the HIRLAM model using a digital filter. *Mon. Wea. Rev.,* **120,** 1019–1034.

——, D. Giard, and V. Ivanovici, 1997: Improving the efficiency of a digital filtering scheme. *Mon. Wea. Rev.,* **125,** 1976–1982.

Machenhauer, B., 1977: On the dynamics of gravity oscillations in a shallow water model with applications on normal mode initialization. *Beitr. Phys. Atmos.,* **50,** 253–271.

Pagé, C., L. Fillion, and P. Zwack, 2007: Diagnosing summertime mesoscale vertical motion: Implications for atmospheric data assimilation. *Mon. Wea. Rev.,* **135,** 2076–2094.

Puri, K., W. Bourke, and R. Seaman, 1982: Incremental linear normal mode initialization in four-dimensional data assimilation. *Mon. Wea. Rev.,* **110,** 1773–1785.

Radnóti, G., and Coauthors, 1995: The spectral limited area model ARPEGE-ALADIN. Research activities in atmospheric and oceanic modelling, PWPR Rep. 7, WMO-TD 699, 111–118.

Sadiki, W., C. Fischer, and J.-F. Geleyn, 2000: Mesoscale background error covariances: Recent results obtained with the limited area model ALADIN over Morocco. *Mon. Wea. Rev.,* **128,** 3927–3935.

Širokà, M., R. Brožkovà, G. Bölöni, C. Fischer, J.-F. Geleyn, and A. Horányi, 2001: Recent experiments with data assimilation in ALADIN/LACE model. *Proc. 23rd EWGLAM/8th SRNWP Meeting,* Krakow, Poland, EUMETNET/C-SRNWP.

Ştefănescu, S., L. Berre, and M. Belo Pereira, 2006: The evolution of dispersion spectra and the evaluation of model differences in an ensemble estimation of error statistics for a limited-area analysis. *Mon. Wea. Rev.,* **134,** 3456–3478.

Termonia, P., 2008: Scale-selective digital-filtering initialization. *Mon. Wea. Rev.,* **136,** 5246–5255.

——, and F. Voitus, 2008: Externalizing the lateral boundary conditions from the dynamic core in semi-implicit semi-Lagrangian models. *Tellus,* **60A,** 632–648.

Voitus, F., P. Termonia, and P. Bénard, 2009: Well-posed lateral boundary conditions for spectral semi-implicit semi-Lagrangian schemes: Tests in a one-dimensional model. *Mon. Wea. Rev.,* **137,** 315–330.